Rencontres GDR - GDM 2023

Phase field modeling of microstructure and cracking pattern formation

Matthieu Degeiter

Introduction

Heterogeneous materials and microstructures : length scales $[10^{-9} ; 10^{-6}]$ m

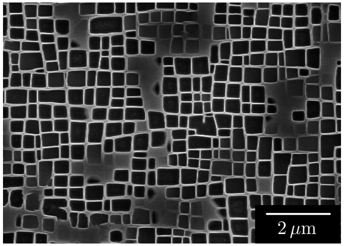

F. Diologent

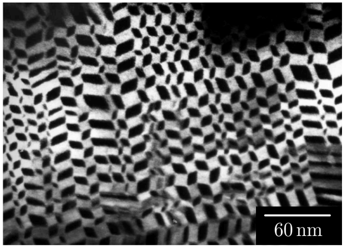

Y. Le Bouar

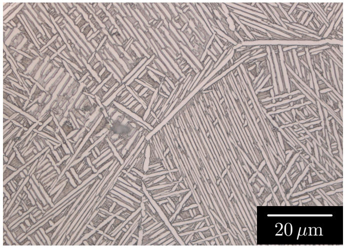

E. Aeby-Gautier et al.

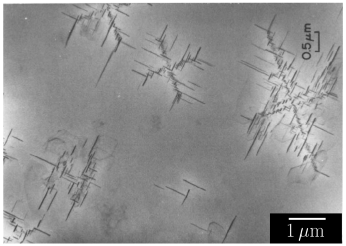

V. Perovic et al.

1. Influence of elasticity on the microstructure of superalloys

Yann Le Bouar[2], Benoît Appolaire[3], Mikael Perrut[1], Alphonse Finel[2]

2. Modeling of cracking in thin films on a stretchable substrate

Umut Salman[4], Damien Faurie[4], Yann Le Bouar[2], Alphonse Finel[2]

Outline

1. Minimal model system
2. Linear stability analysis
3. Phase field modeling

[1] SIAM DMAS, ONERA
[2] LEM DMAS, ONERA-CNRS
[3] IJL Université de Lorraine-CNRS
[4] LSPM Université Sorbonne Paris Nord-CNRS

1. Introduction

Single-crystal superalloys

- Excellent mechanical properties at high temperature
- Design of high pressure turbine blades in gas turbines

Microstructure

Strengthened by precipitation of γ' phase (precipitates) in the γ phase (matrix)

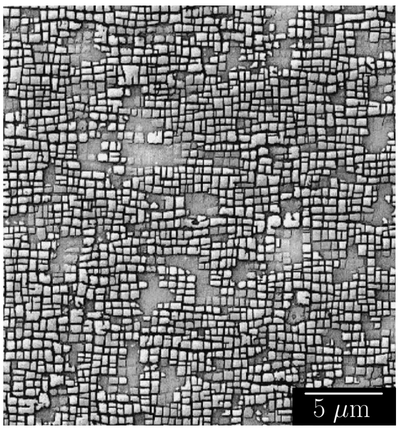

Epishin et al., Acta Mat., 2000

In service

Microstructure evolution degrades the blade properties

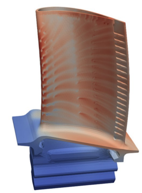

Temperature

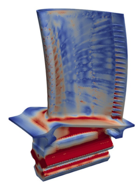

Von Mises stress

Daniel et al., 2022

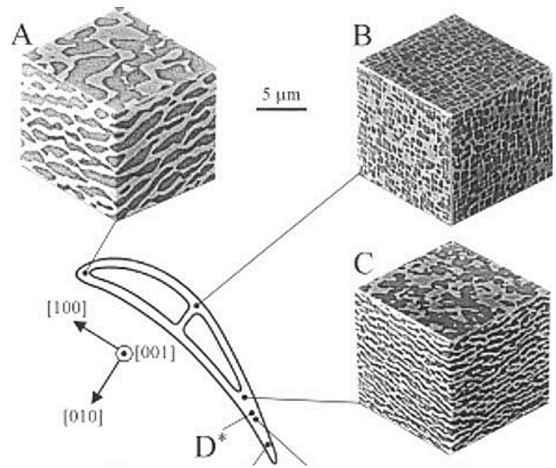

Von Grossman et al., 1998

Microstructure modeling at the scale of the blade

1. Introduction

Equilibrium phase diagram : binary nickel (Ni) and aluminium (Al) mixture

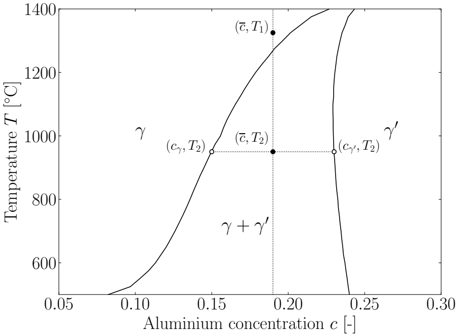

- given composition $\bar{c}$ at temperature T_1
- decrease temperature $T_1 \rightarrow T_2$
- precipitation $\gamma \rightarrow \gamma + \gamma'$
- equilibrium concentrations c_γ and $c_{\gamma'}$

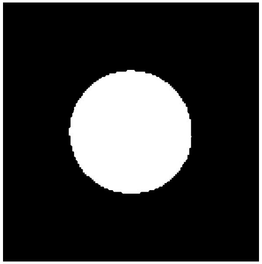

Misfit $\delta a/a$ between lattice parameters : difference in local order induce atomic size effects

γ phase

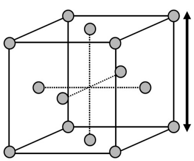

$a_\gamma > a_{\gamma'}$

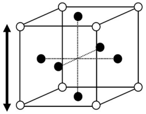

γ' phase

$$\delta a/a = 2\frac{a_{\gamma'} - a_\gamma}{a_{\gamma'} + a_\gamma}$$

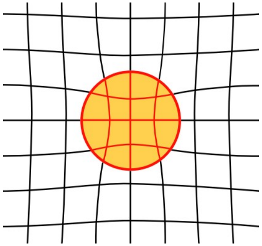

Precipitation $\gamma \rightarrow \gamma + \gamma'$: solid-state phase transformation

- first order phase transition driven by diffusion
- difference in local order generates a strain field

1. Introduction

Cubic anisotropy : precipitate shapes and arrangement strongly influenced by elasticity

Equilibrium shape of an isolated precipitate

- Competition between interface and strain energies
- Shape transition during precipitate growth

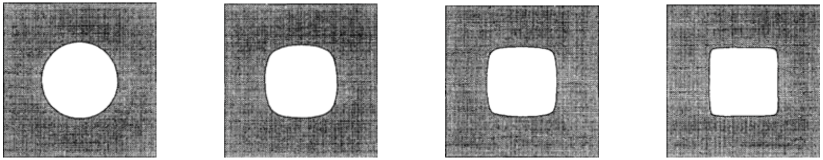

M.E. Thompson, C.S. Su, P.W. Voorhees, 1994

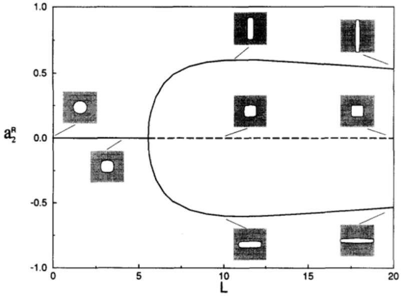

Elastic interactions among precipitates : long-range and strongly anisotropic

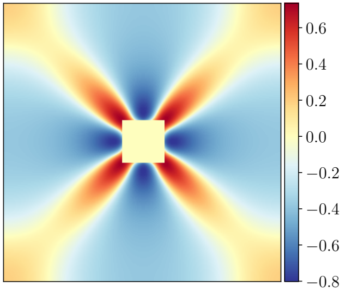

Elastic interaction energy

- Precipitate alignments along cubic soft directions
- Interactions induce deviations from the equilibrium shape

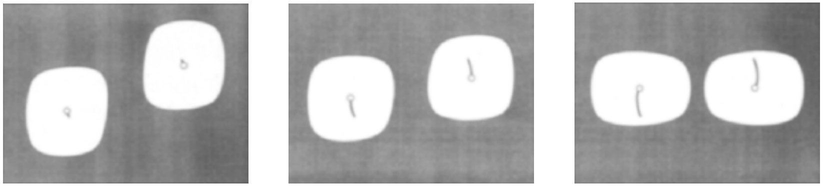

C. H. Su, P. W. Voorhees, Acta Mat., 1996

1. Introduction

Cuboid shapes and precipitate alignments in γ/γ' microstructure :

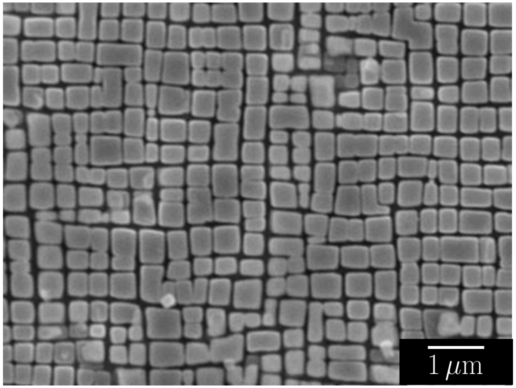

D. Texier, Université de Toulouse, 2013

Question: origin of the $\gamma-$ and $\gamma'-$ dislocation patterns in the microstructure ?

Outline:

1.1 Model presentation

1.2 Stability analysis

1.3 Phase field modeling

1.1 Model presentation

Minimal model system : effective Ni-Al binary alloy at composition $\bar{c}$ and temperature T_2

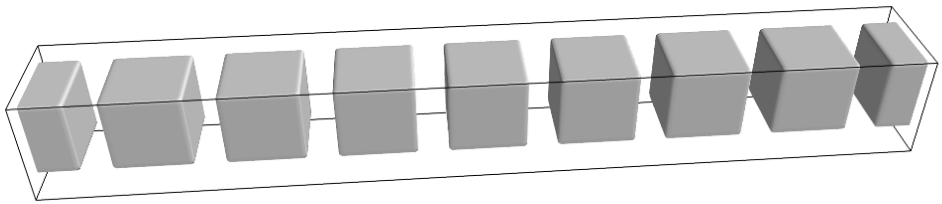

Fields and description

- concentration $c(\boldsymbol{r}, t)$
- displacement $u_i(\boldsymbol{r}, t)$

Constants

- eq. concentrations
- interface energy σ (J.m^{-2})
- diffusion coefficient D (m^2.s^{-1})
- eigenstrain ε_0
- elastic constants λ_{ijkl} (J.m^{-3})

Small strains

$$\varepsilon^{el}_{ij}(\boldsymbol{r}) = \bar{\varepsilon}_{ij} + \delta\varepsilon_{ij}(\boldsymbol{r}) - \varepsilon^0_{ij}(\boldsymbol{r})$$

$$\delta\varepsilon_{ij}(\boldsymbol{r}) = \frac{1}{2}\left(\frac{\partial \delta u_i}{\partial r_j} + \frac{\partial \delta u_j}{\partial r_i}\right)$$

Assumptions

- homogeneous elasticity
- constant temperature
- no mechanical loading

1.1 Model presentation

Minimal model system : effective Ni-Al binary alloy at composition $\bar{c}$ and temperature T_2

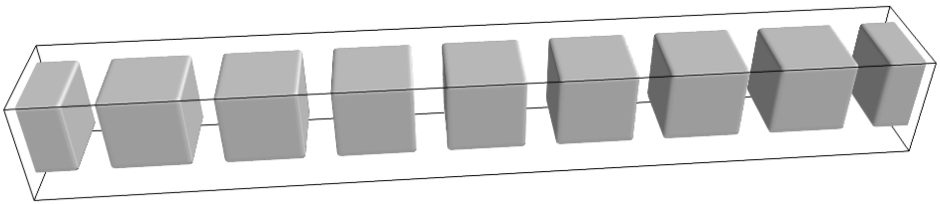

Free energy functional

$$F = \int_V f_{ch}(c) + f_{el}(\varepsilon_{ij}^{el}, c)\, dV$$

Chemical energy density

$$f_{ch}(c) = f(c) + \frac{\lambda}{2}|\nabla c|^2$$

$$f(c) = A(c - c_\gamma)^2 (c - c_{\gamma'})^2$$

Strain energy density

$$f_{el}(\varepsilon_{ij}^{el}, c) = \frac{1}{2}\,\lambda_{ijkl}\,\varepsilon_{ij}^{el}(c)\,\varepsilon_{kl}^{el}(c)$$

Elastic equilibrium

$$\frac{\delta F}{\delta \bar{\varepsilon}_{ij}} = 0 \quad ; \quad \frac{\delta F}{\delta(\delta u_i(\boldsymbol{r}))} = 0$$

Cahn-Hilliard equation

$$\frac{\partial c}{\partial t} = M \nabla^2 \frac{\delta F}{\delta c}$$

Elastic relaxation time $\ll$ characteristic time for diffusion

1.2 Stability analysis

A.G. Khachaturyan, 1983, A.G. Khachaturyan, V. M. Airapetyan, *Phys. Stat. Sol.(a)*, 1974

Origin of alignment defects ?

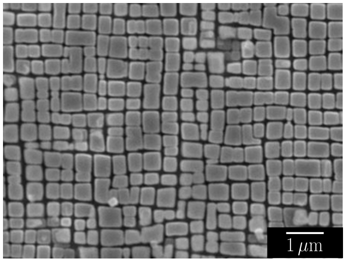

D. Texier, Université de Toulouse, 2013

Cubic distribution of spherical inclusions

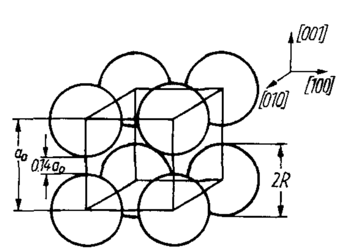

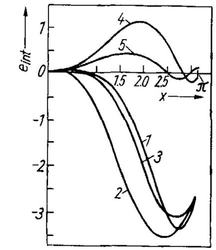

A.G. Khachaturyan, V. M. Airapetyan, Phys. Stat. Sol.(a), 1974

Strain energy in direct space

$$F_{el} = \frac{1}{2}\int_V \lambda_{ijkl}\left(\varepsilon_{ij}(\boldsymbol{r}) - \varepsilon^0_{ij}\theta(\boldsymbol{r})\right)\left(\varepsilon_{kl}(\boldsymbol{r}) - \varepsilon^0_{kl}\theta(\boldsymbol{r})\right) dV$$

Shape function

$$\theta(\boldsymbol{r}) = \sum_{\boldsymbol{R}} \theta_0(\boldsymbol{r} - \boldsymbol{R})$$

Strain energy in Fourier space

$$F_{el} = \frac{V}{2}\sum_{\boldsymbol{q}} B(\boldsymbol{q}/q)|\theta(\boldsymbol{q})|^2$$

$$F_{el} = \frac{V}{2}\sum_{\boldsymbol{q}} B(\boldsymbol{q}/q)|\theta_0(\boldsymbol{q})|^2 \sum_{\boldsymbol{R},\boldsymbol{R}'} e^{-\mathrm{i}\boldsymbol{q}(\boldsymbol{R}-\boldsymbol{R}')}$$

1.2 Stability analysis

A.G. Khachaturyan, V. M. Airapetyan, *Phys. Stat. Sol.(a)*, 1974

Origin of alignment defects ?

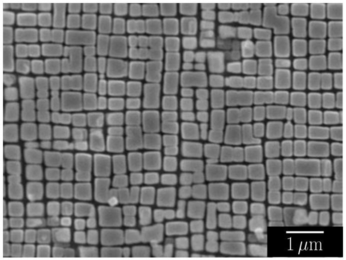

D. Texier, Université de Toulouse, 2013

Stability wrt. small perturbation : $\boldsymbol{R} = \boldsymbol{R}_0 + \boldsymbol{u}(\boldsymbol{R}_0)$

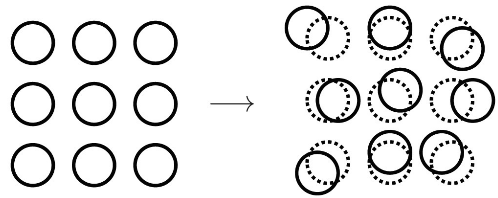

Energy variation

- $\delta^2 F > 0 \;\; \Rightarrow$ stable wrt. perturbation
- $\delta^2 F < 0 \;\; \Rightarrow$ unstable wrt. perturbation

Second variation

$$\delta^2 F = \frac{1}{2} \sum_{\boldsymbol{\tau}} \kappa_{ij}(\boldsymbol{\tau})\; u_i(\boldsymbol{\tau})\; u_j^*(\boldsymbol{\tau})$$

High symmetry directions

- $\Gamma(0,\, 0,\, 0)$
- $X(\pi/a,\, 0,\, 0)$
- $M(\pi/a,\, \pi/a,\, 0)$
- $R(\pi/a,\, \pi/a,\, \pi/a)$

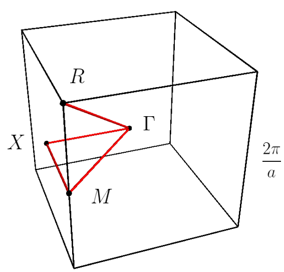

Microstructure properties

- $a = 350$ nm
- $\tau_{\gamma'} = 0.37$
- $\varepsilon_0 = 0.48\%$
- $c_{11} = 250$ GPa
- $c_{12} = 160$ GPa
- $c_{44} = 118.5$ GPa

1.2 Stability analysis

Cubic arrangement of spherical precipitates

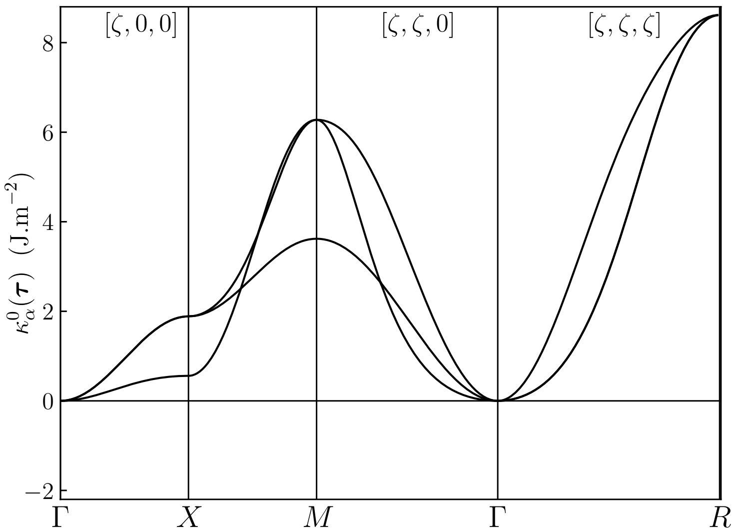

Spectrum of hessian eigenvalues

1.2 Stability analysis

Cubic arrangement of spherical precipitates

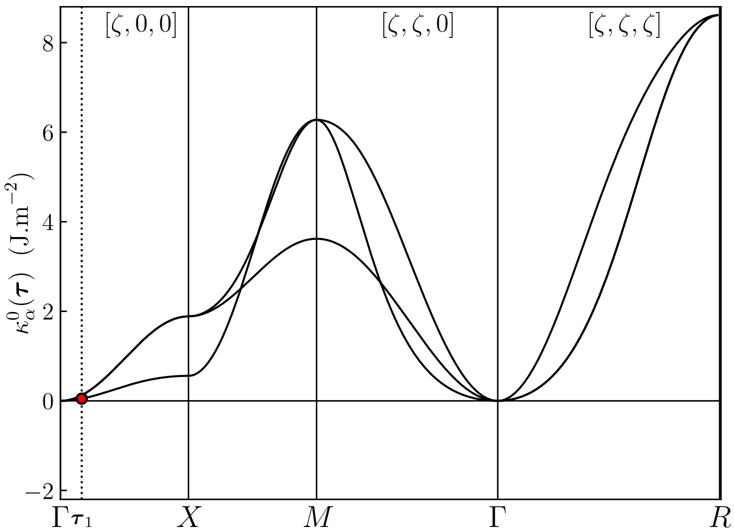

Spectrum of hessian eigenvalues

Perturbation mode

- longitudinal $\boldsymbol{\tau}_1(\zeta, 0, 0)$, $\zeta = 2\pi/12a$

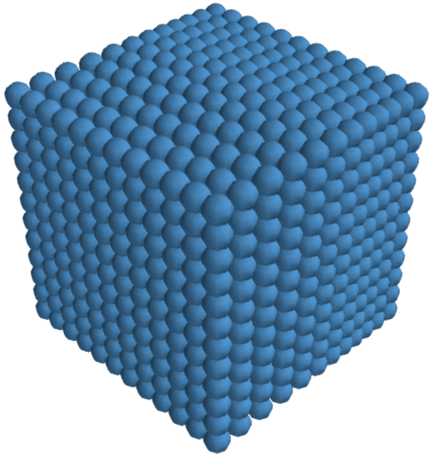

1.2 Stability analysis

Cubic arrangement of spherical precipitates

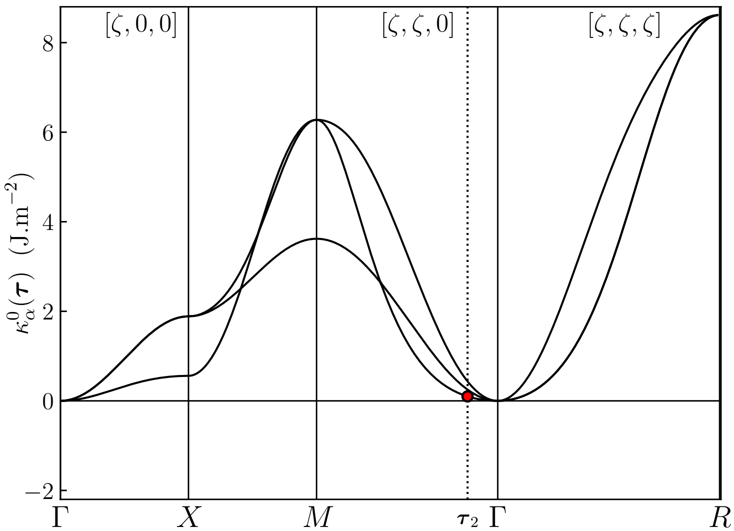

Spectrum of hessian eigenvalues

Perturbation mode

- transverse $\boldsymbol{\tau}_2(\zeta, \zeta, 0)$, $\zeta = 2\pi/12a$

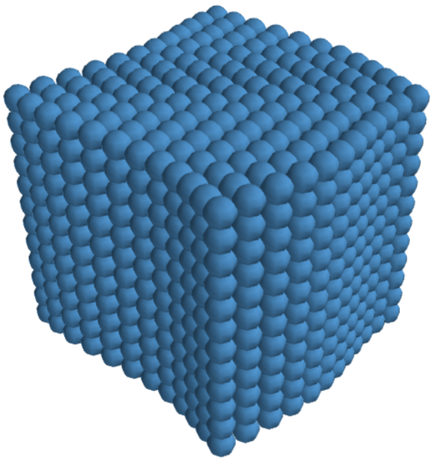

1.2 Stability analysis

Cubic arrangement of spherical precipitates

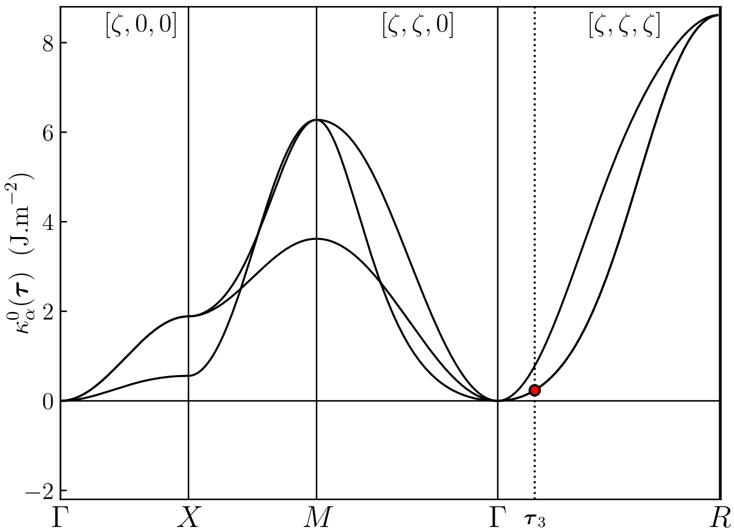

Spectrum of hessian eigenvalues

Perturbation mode

- transverse $\boldsymbol{\tau}_3(\zeta,\zeta,\zeta)$, $\zeta = 2\pi/12a$

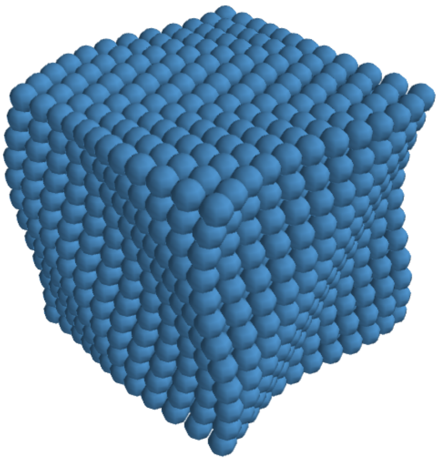

1.2 Stability analysis

Cubic arrangement of spherical precipitates

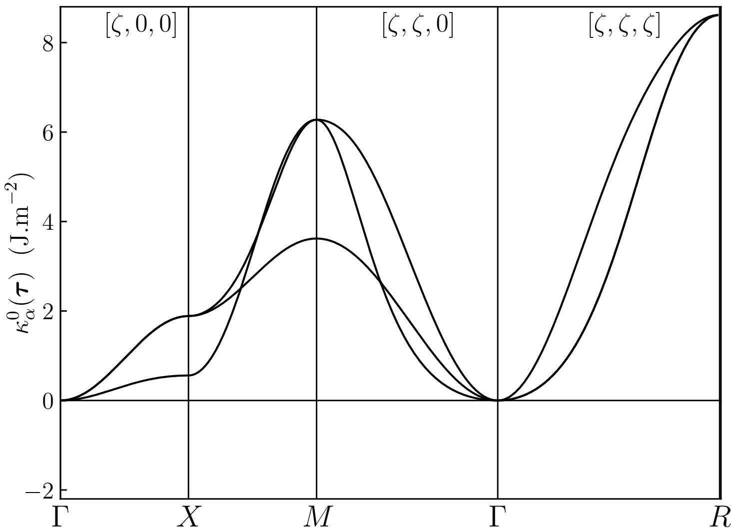

Spectrum of hessian eigenvalues

System stability

- $\delta^2 F > 0$ for any $\boldsymbol{\tau}$ on the path
- Khachaturyan and Airapetyan
- stable arrangement at $\tau_{\gamma'} = 0.37$

Hypothesis of spherical precipitates

- cubic shape?

1.2 Stability analysis

Cubic arrangement of cubic precipitates

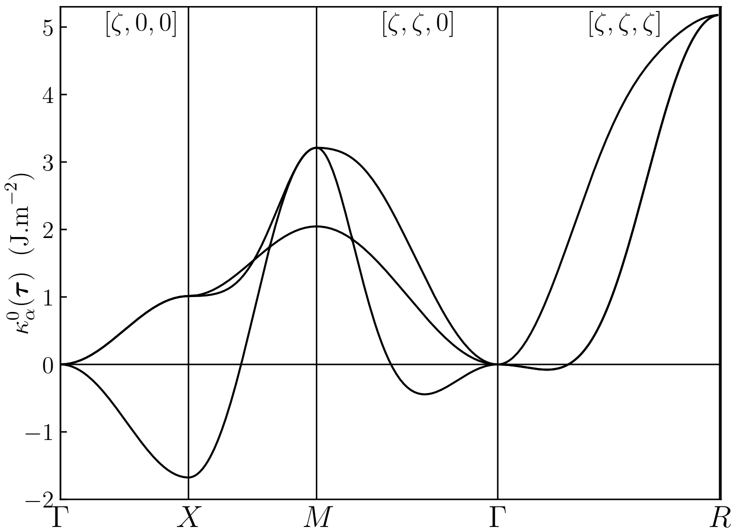

Spectrum of hessian eigenvalues

1.2 Stability analysis

Cubic arrangement of cubic precipitates

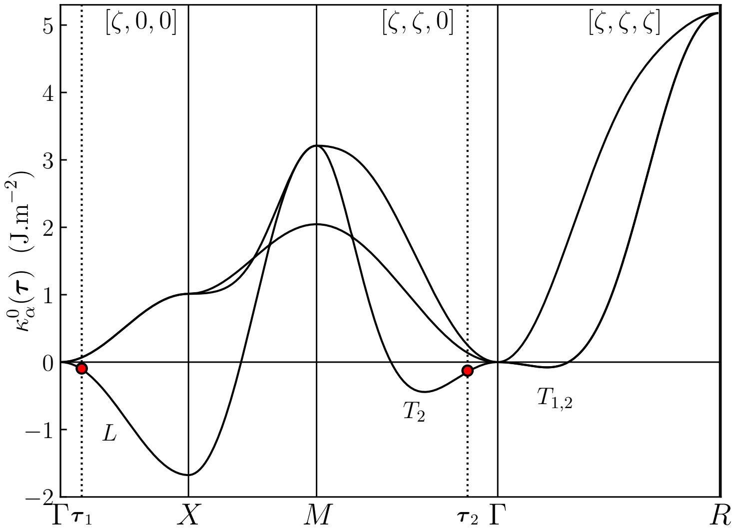

Spectrum of hessian eigenvalues

Most unstable branches

- longitudinal L $(\zeta,0,0)$, $\zeta = 2\pi/12a$

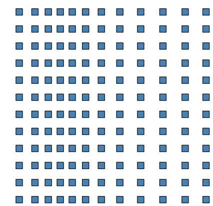

- transverse T_2 $(\zeta,\zeta,0)$, $\zeta = 2\pi/12a$

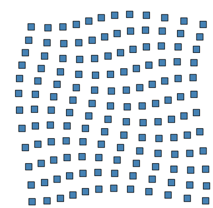

1.3 Phase field modeling

Perturbation $L\,(\zeta, 0, 0)$

- $\zeta = 2\pi/8a$
- amplitude 28.8 nm

Remarks

- shape changes
- no precipitate migration

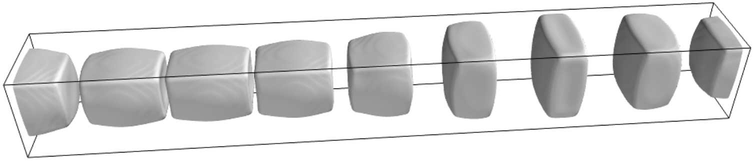

Eckhaus instability in pattern formation: defect creation

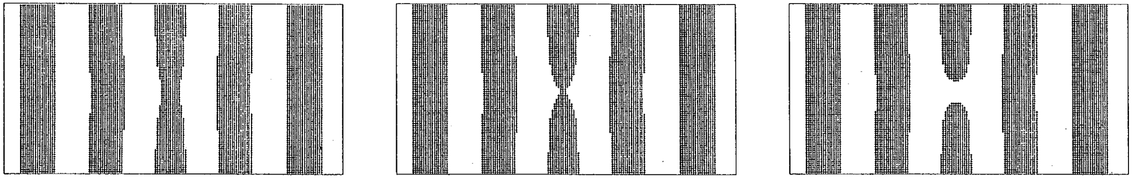

H. Sakaguchi, Prog. Theor. Phys., 1991

Longitudinal instability: formation of γ- and γ'-dislocations?

RÉPUBLIQUE FRANÇAISE

ONERA

THE FRENCH AEROSPACE LAB

1.3 Phase field modeling

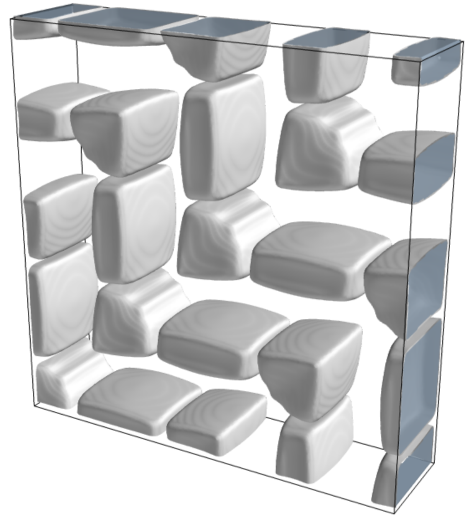

Perturbation T_2 $(\zeta, \zeta, 0)$

- $\zeta = 2\pi/4a$
- amplitude 36 nm

Remarks

- shape changes
- no precipitate migration

Formation of chevron patterns

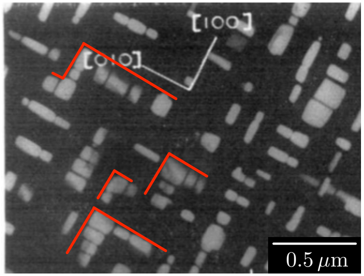

Ardell et al., Acta Metall., 1966

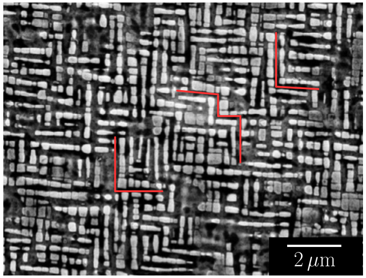

X. Li et al., J. Alloys. Compd., 2015

1. Recap and prospects

Recap

- Instability of the cubic arrangement of cubic precipitates
- Development of instabilities and formation of alignment defects

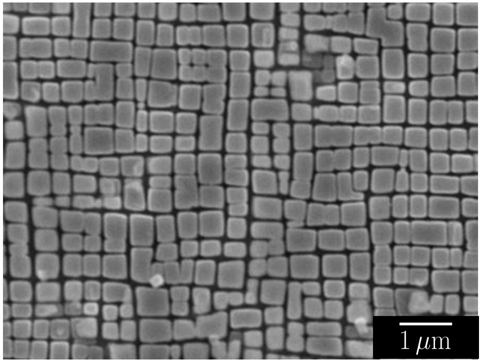

D. Texier, Université de Toulouse, 2013

Prospects

- Shape and arrangement perturbations in stability analysis
- Coupling between stable and unstable modes

Modeling of cracking of thin films on a stretchable substrate

2. Introduction

Flexible electronics: lighting, sensors, solar panels, ...

osram-oled.com

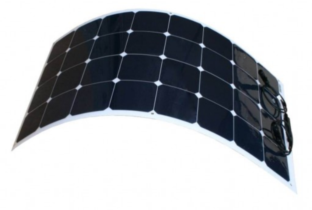

sellande.com

- brittle film $h_F \sim 100\text{nm}$
- stretchable substrate $h_S \sim 1000 \times h_F$
- functional properties

Uniaxial mechanical loading

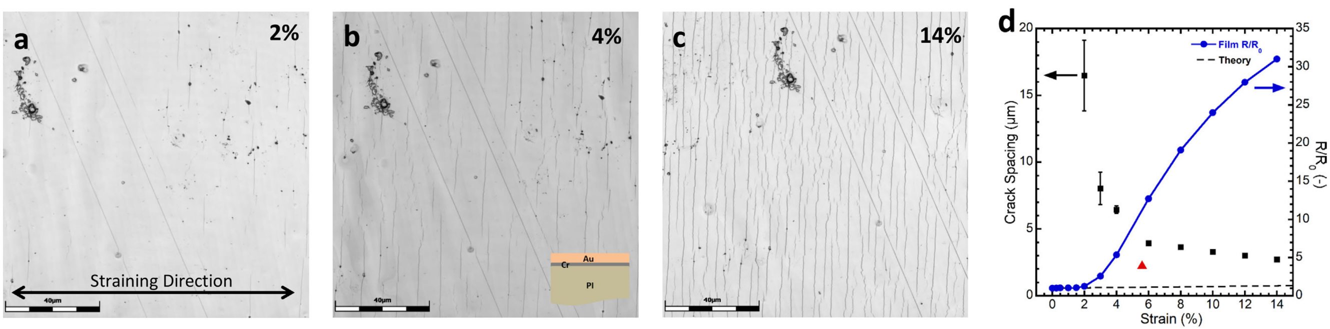

M. J. Cordill et al., Frontiers in Materials, 2016.

Significant increase in the film electrical resistance

2. Introduction

Biaxial mechanical loading

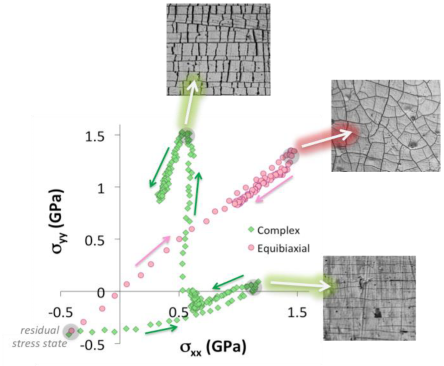

D. Faurie et al., Acta Mat. 2019

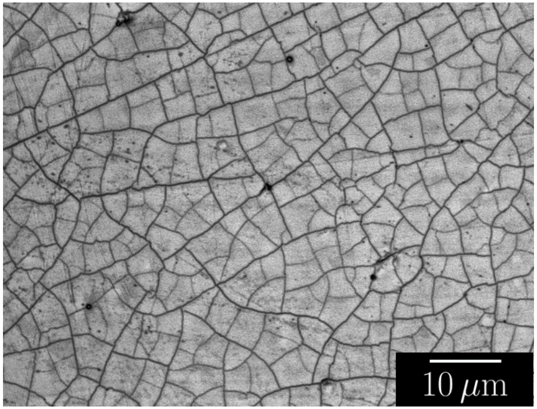

D. Faurie et al., 2021

Outline:

2.1 Model presentation

2.2 Stability analysis

2.3 Phase field modeling

2.1 Model presentation

Minimal system

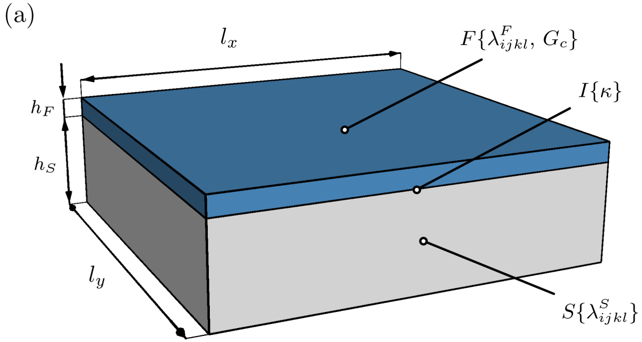

Fields and description

- film damage α
- displacements $u_i(\boldsymbol{r})$

Constants

- G_c fracture energy (J.m^{-2})
- λ^X_{ijkl} isotropic elastic constants (J.m^{-3})
- κ interface stiffness (J.m^{-4})

Small strains

$$u_i(\boldsymbol{r}) = \bar{\varepsilon}_{ij} r_j + \delta u_i(\boldsymbol{r})$$
$$\varepsilon_{ij}(\boldsymbol{r}) = \bar{\varepsilon}_{ij} \quad + \delta\varepsilon_{ij}(\boldsymbol{r})$$

$$\delta\varepsilon_{ij}(\boldsymbol{r}) = \frac{1}{2}\left(\frac{\partial \delta u_i}{\partial r_j} + \frac{\partial \delta u_j}{\partial r_i}\right)$$

Assumptions

- $l_x, l_y \gg (h_F + h_S)$ and PBC
- no delamination or plasticity

2.1 Model presentation

Minimal system

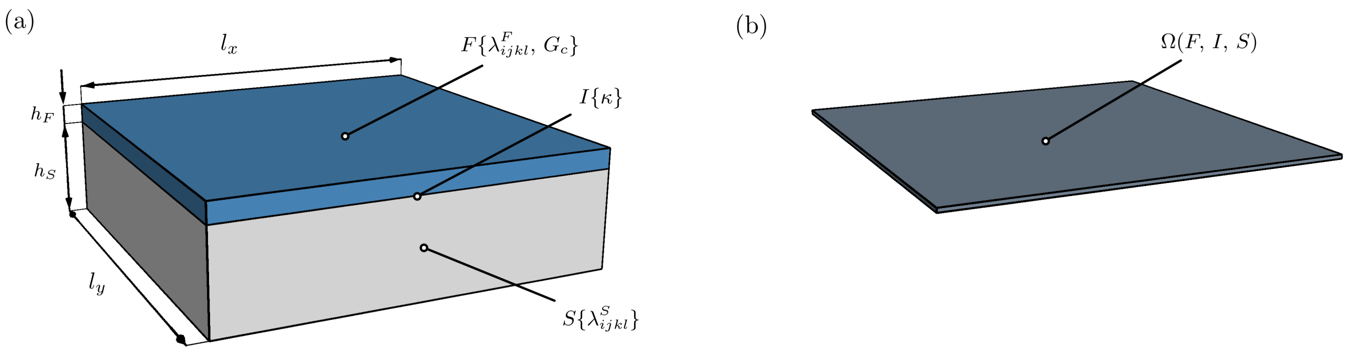

Functional

$$F = \int_\Omega h_F \times \left[f^F_{frac}(\alpha) + f^F_{el}(\varepsilon^F_{ij}, h(\alpha)) \right] + h_S \times f^S_{el}(\varepsilon^S_{ij}) + f^I_{bond}(u^F_i, u^S_i)\, d\Omega$$

Fracture energy density

B. Bourdin, G.A. Francfort, J.-J. Marigo, JMPS, 2000.

$$f^F_{frac}(\alpha) = \frac{G_c}{4\ell}\left(\alpha^2 + 4\ell^2|\nabla\alpha|^2\right) \quad ; \quad h(\alpha) = (1-\alpha)^2$$

Film strain energy density : for isotropic λ^F_{ijkl}

C. Miehe, et al., Int. J. Num. Meth. Eng., 2010.

$$f^F_{el}(\varepsilon^F_{ij}, h(\alpha)) = h(\alpha) f^{F+}_{el}(\varepsilon^F_{ij}) + f^{F-}_{el}(\varepsilon^F_{ij})$$

Bonding energy density

$$f^I_{bond}(u^F_i, u^S_i) = \frac{\kappa}{2}(u^F_i - u^S_i)^2$$

Substrate strain energy density

$$f^S_{el}(\varepsilon^S_{ij}) = \frac{1}{2}\lambda^S_{ijkl}\varepsilon^S_{ij}\varepsilon^S_{kl}$$

2.1 Model presentation

Minimal system

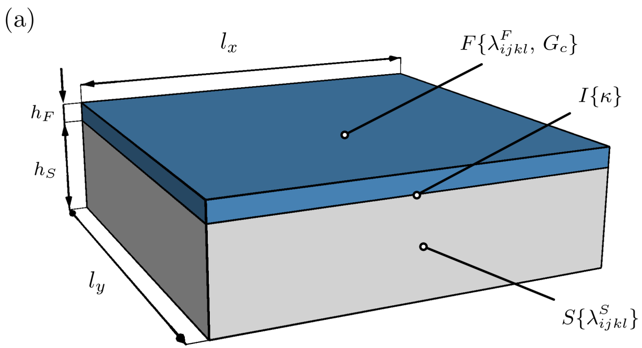

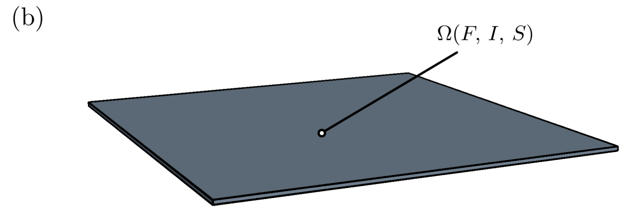

Equilibrium equations

$$\frac{\delta F}{\delta(\delta u_i^X(\boldsymbol{r}))} = 0$$

$$\frac{\delta F}{\delta \alpha(\boldsymbol{r})} = 0$$

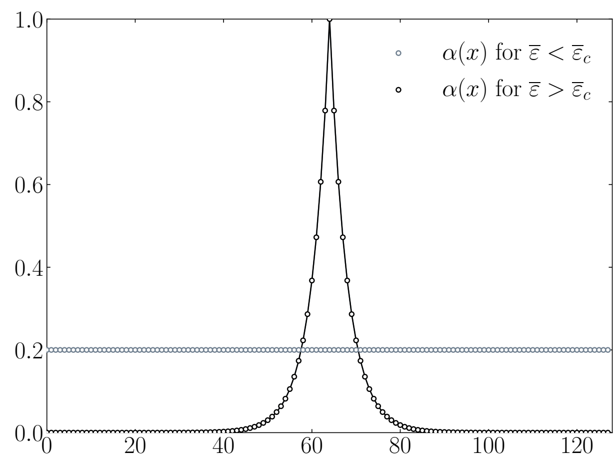

2.2 Stability analysis

1D system **O.U. Salman, L. Truskinovsky, JMPS, 2021.**

Homogeneous solution at equilibrium

$$\phi_0 = {}^T(\alpha_0, u^X)$$

Energy variation around ϕ_0

- $\delta^2 F > 0 \quad \Rightarrow \quad$ stable wrt. perturbation
- $\delta^2 F < 0 \quad \Rightarrow \quad$ unstable wrt. perturbation

System properties

- $d = 10^{-6}$ m
- $\ell = 2d$
- $h_F = 0.25d$
- $h_S = 100 h_F$
- $G_c = 100$ J.m^{-2}
- $E_F = 200 \times 10^9$ J.m^{-3}
- $E_S = 100 \times 10^9$ J.m^{-3}
- $\kappa = 7.5 \times 10^{13}$ J.m^{-4}

Stability wrt. small perturbation

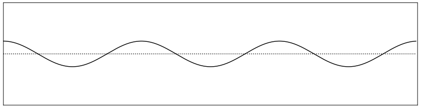

Second variation

$$\delta^2 F = \frac{1}{2} \sum_q H_{ij}(q)\, \delta\phi_i(q)\, \delta\phi_j^*(q)\ , \ \delta\phi_i \in \{\alpha, \delta u^X\}$$

Smallest $H_{ij}(q)$ eigenvalues

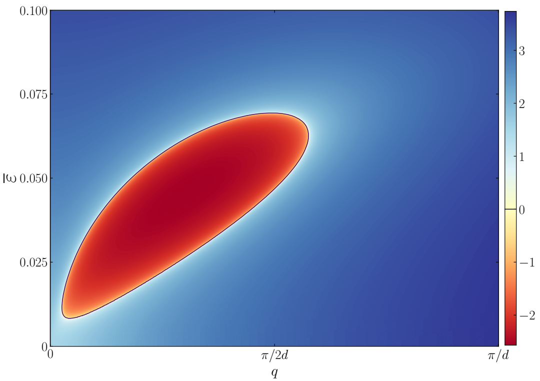

2.2 Stability analysis

2D system

Homogeneous solution at equilibrium

$$\phi_0 = {}^T(\alpha_0, u_1^X, u_2^X)$$

Second variation

$$\delta^2 F = \frac{1}{2} \sum_{\boldsymbol{q}} H_{ij}(\boldsymbol{q})\, \delta\phi_i(\boldsymbol{q})\, \delta\phi_j^*(\boldsymbol{q})\ ,\ \delta\phi_i \in \{\delta\alpha, \delta u_1^X, \delta u_2^X\}$$

Hessian determinant : representation of $\det H(\boldsymbol{q})$ close to the onset of instability $\bar{\varepsilon} \simeq \bar{\varepsilon}_c$

Equibiaxial loading $\bar{\varepsilon}_{22} = \bar{\varepsilon}_{11} = \bar{\varepsilon}$

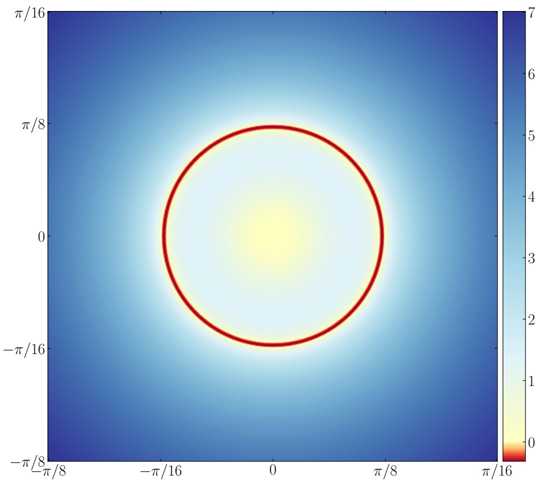

Quasi-uniaxial loading $\bar{\varepsilon}_{11} = \bar{\varepsilon}$, $\bar{\varepsilon}_{22} = 0.2\bar{\varepsilon}$

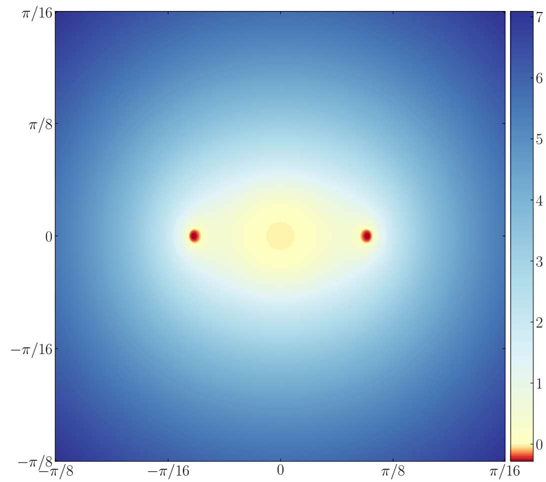

Phase field modeling

Stability analysis: hessian determinant

- $l_x = 512d$; $l_y = 512d$
- $G_c = 100$ J.m^{-2}
- $E_F = 200 \cdot 10^9$ J.m^{-3}
- $E_S = 4 \cdot 10^9$ J.m^{-3}
- $\kappa = 1 \cdot 10^{13}$ J.m^{-4}

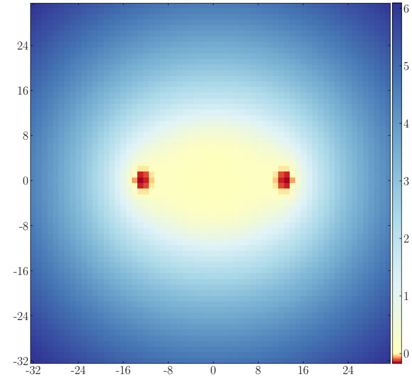

Computed damage field close to the onset of instability

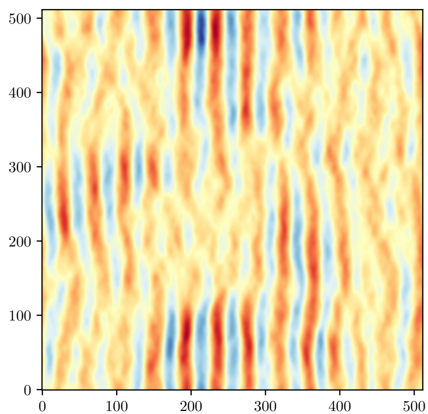

$\delta\alpha(\mathbf{r}) = \alpha(\mathbf{r}) - \langle\alpha(\mathbf{r})\rangle$

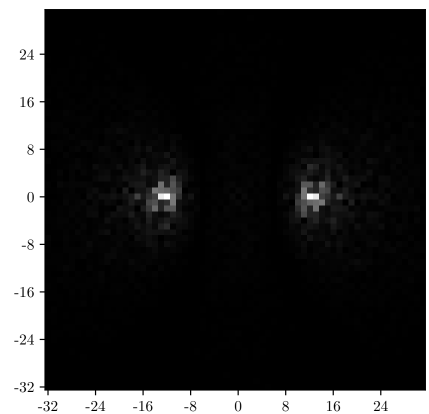

$|\delta\alpha(\mathbf{q})| = |\mathcal{F}\{\delta\alpha(\mathbf{r})\}|$

Université Sorbonne Paris Nord
Université de Paris
ONERA
THE FRENCH AEROSPACE LAB

Phase field modeling

Stability analysis: hessian determinant

- $l_x = 512d$; $l_y = 512d$
- $G_c = 100$ J.m^{-2}
- $E_F = 200 \cdot 10^9$ J.m^{-3}
- $E_S = 4 \cdot 10^9$ J.m^{-3}
- $\kappa = 1 \cdot 10^{13}$ J.m^{-4}

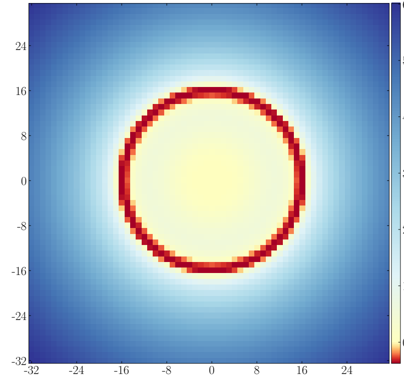

Computed damage field close to the onset of instability

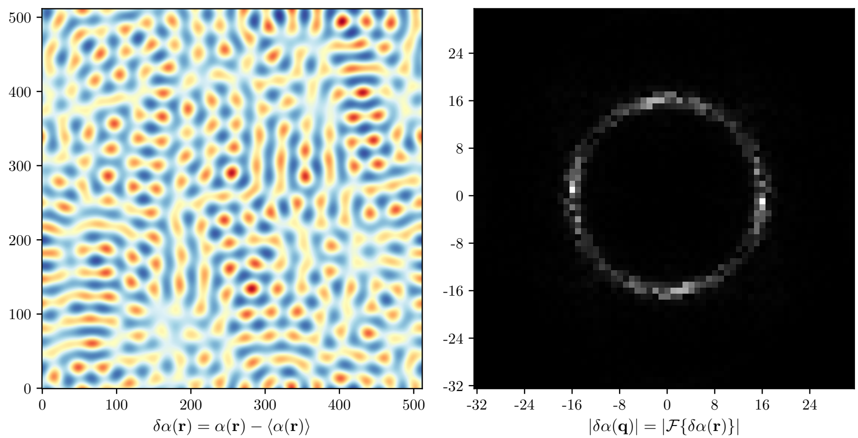

Phase field modeling

Thin film cracking : evolution of displacement u_1 and damage α fields

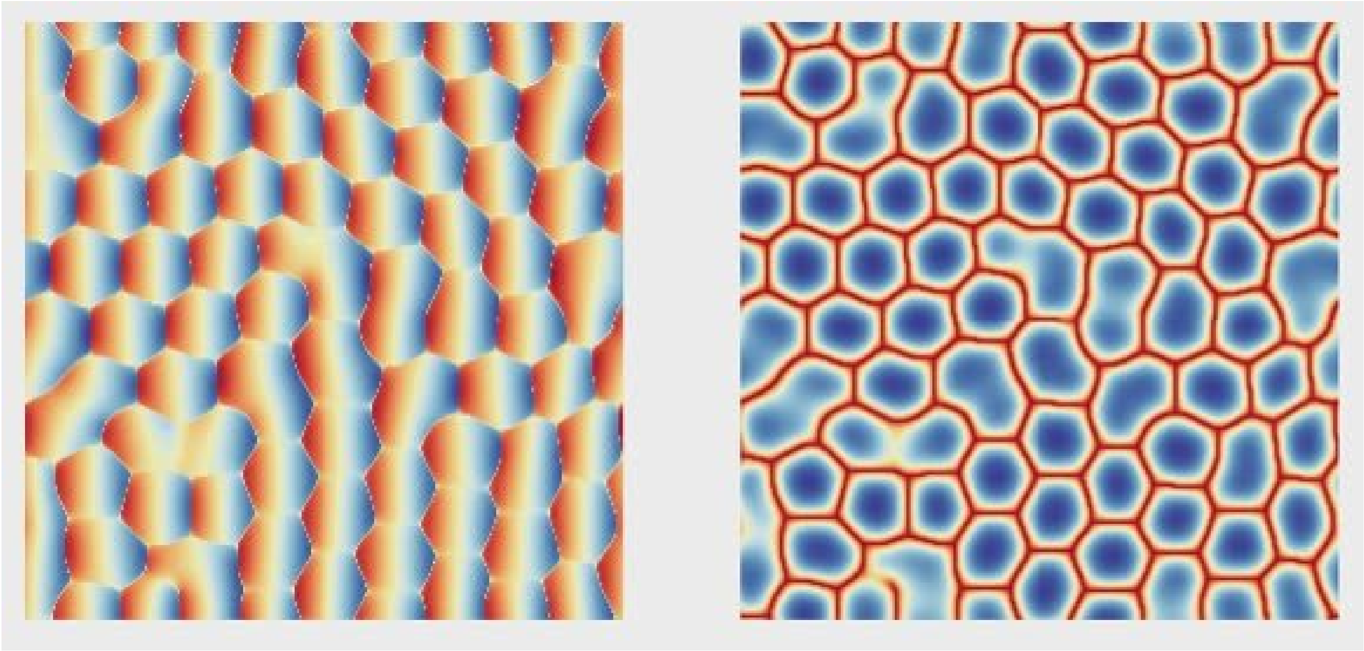

2. Recap and prospects

Recap

- Stability analysis of brittle thin films on deformable substrate
- Instability selection and formation of crack patterns with phase field modeling

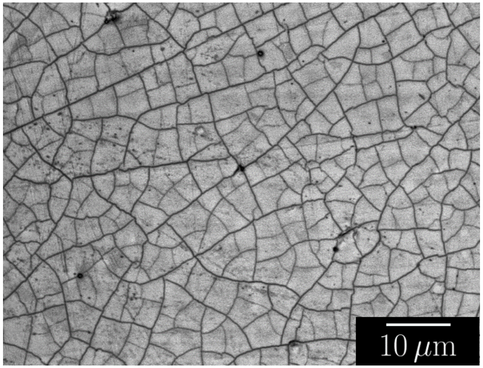

D. Faurie et al., Université Sorbonne Paris Nord, 2021

Prospects

- Plasticity in the substrate, buckling and delamination of the film
- Phase diagram of crack patterns

Merci pour tout !

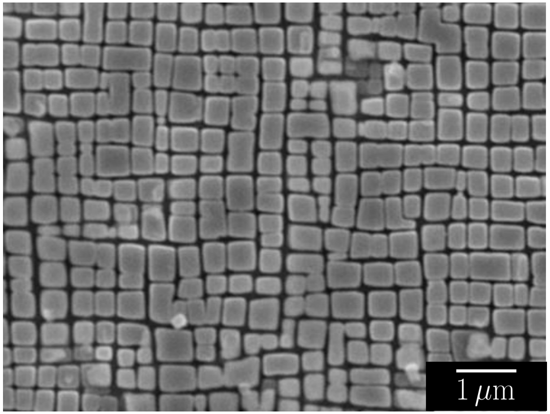

D. Texier, Université de Toulouse, 2013

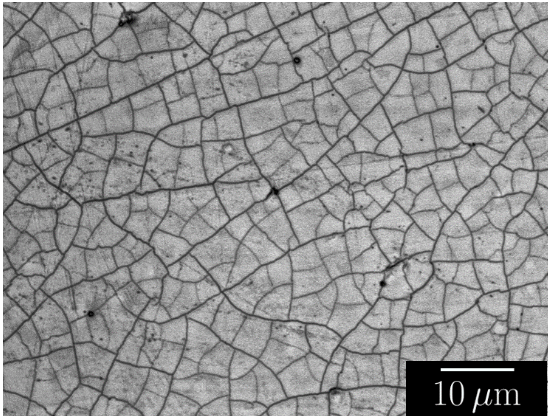

D. Faurie et al., Université Sorbonne Paris Nord, 2021